CHAPTER 6

HEXAVALENT CHROMIUM REMOVAL USING BI-FUNCTIONAL NANOCOMPOSITE MEMBRANES

An innovative approach has been used to synthesize cost-effective bi-functional membranes for removing Cr(VI) from wastewater through reduction to Cr(III) and separation with the help of a membrane. Conditions governing the separation process such as- pH, particle loading, and concentration of Cr(VI) have been optimized to maximize the % rejection and photo-catalytic reduction to Cr(III). Through the use of RSM it has been observed that rejection of 91.58% and reduction of 87.02% are possible at the predicted pH (5.55), particle loading (2.14%) and Cr (VI) concentration (25mg/L). With actual industrial effluent >90% rejection and 85% reduction were achieved.

6.1 INTRODUCTION

Chromium, a highly toxic heavy metal, exists as trivalent chromium Cr (III)) and hexavalent chromium Cr (VI). The Cr (VI) is environmentally more hazardous compared to Cr(III) and is toxic not only to humans but also to flora and fauna (Jyothi et al. 2017). It is considered as one of the top twenty significant contaminants in the priority list of hazardous substances. The potential sources of Cr (VI) discharge into water bodies are leather tanning, metal finishing, electroplating, etc. (Zang et al. 2020). The governments and regulatory organizations are applying strict regulation on industries to limit their Cr(VI) bearing discharges. The U. S. Environmental Protection Agency (USEPA) has set 100 μg/L as the maximum contamination level (MCL) for total Cr in drinking water, whereas the World Health Organization (WHO) has recommended a maximum allowable concentration of 50 μg/L (Jyothi et al., 2017). So it has become crucially important to

control the high level of carcinogenic and toxic Cr (VI) released from different industries to maintain the effluent wastewater quality according to the permissible standard. Various conventional technologies like adsorption, ion exchange, and electrochemical reduction used for the elimination of Cr (VI) have several drawbacks like ineffective removal of metal at low concentration, increased volume of sludge generation and difficulty in their disposal (secondary pollutant generation), high chemical consumption, relatively high operational cost, non-destructive process, and incompatibility for large-scale application are their major limitations (Crini and Lichtfouse 2019, Burakov et al., 2018).

In contrast, the emerging technologies like ion-exchange, electro-dialysis, reverse osmosis, and photo-catalysis have effective removal capacity as well as low sludge volume production. But these are expensive (Barakat and Schimdt 2010). Poor recovery of directly used photo-catalyst limits its successful application in suspended form (Jyothi et al. 2017). In comparison, photo-catalytic membrane technology is a single-step treatment procedure that doesn't require chemicals and removes the toxic metal from wastewater, and retreats the feed wastage (retentate) using the same membrane as photo-catalyst. The development of photocatalytic membrane involves immobilization of catalytic materials on polymer matrix (Ramasundaram et al. 2016). This synergistic effect will enhance the reusability of material and eliminate the generation of a secondary pollutant.

Among the various pressure driven processes, ultrafiltration (UF) has several advantages such as lower energy requirement compared to nano-filtration (NF) and reverse osmosis (RO) (Choudhary et al. 2018). Polyvinylidene fluoride (PVDF) UF membranes have wide commercial applications due to their outstanding resistivity to organic and inorganic acids (Arif et al. 2019). However, high hydrophobicity of PVDF adversely affects the performance of the membrane. Techniques like graft polymerization, chemical grafting,

and physical blending had been adopted to increase hydrophilicity, but weak interaction between the host matrix and filler diminishes the life span of composite material (Arif et al. 2019). Immobilization of inorganic particles (photo-catalyst) into polymer matrix enhances the flux and improves the self-cleaning property of membrane.. Nano-sized titanium dioxide (TiO_2) is widely used as inorganic filler because of its easy processing ability, super hydrophilicity and catalytic-activity (Ramasundaram et al. 2016; Sharma et al. 2017; Mittal et al. 2015).

In this chapter PVDF/TiO_2 NPs composite membranes with different loadings of green synthesized TiO_2 NPs embedded in PVDF polymer were prepared to be used as a photo-catalytic membrane to eliminate toxic Cr (VI) from wastewater and reduce it to Cr (III). This treatment technology prevents the waste production, minimizes the feed wastage and simultaneously reducing the human capital without compromising its efficiency. Insufficient published information is available in the open literature on the application of bi-functional photo-catalyst membranes for the rejection and reduction of Cr (VI) species. At the same time mathematical tool the response surface methodology (RSM) has been used for the first time to optimize the operating parameters governing operation of a bi-functional membrane.

In view of this an attempt has been made to conduct and formulate mathematical predictive models to optimize the governing process conditions (pH, particle loading, Cr concentration) using the response surface methodology (RSM) tool to analyze its outcome on the response (% rejection and % reduction). This methodology reduces the number of experiments and optimizes the parameter to achieve maximum rejection and reduction using the same material. The statistical technique was also employed to obtain the optimum process conditions with remarkable improvement in % rejection and % reduction. After

optimization photo-catalytic composite membranes at the suggested optimized conditions was further used to treat real industrial wastewater high in Cr concentration to further validate the applicability of the developed membrane.

6.2 EXPERIMENTAL PROCEDURE

6.2.1Material

Potassium dichromate and diphenylcarbazide were purchased from Merck (Bombay), Double distilled water (DD) prepared in the laboratory was used in all experiments.

6.2.2 Synthesis of TiO_2 nanoparticles (NPs) and PVDF/TiO_2 composite membrane preparation

The nano-particles and membranes were synthesized as described earlier in Chapter 3 Section 3.2.2 a and 3.2.2.b.

6.2.3 Characterization

The morphological changes before and after Cr removal was studied using Fourier Transform spectroscopy (FTIR) of TIR (02) (Perkin Elmer, Bruker, US) whereas the surface area of the film was analyzed using surface area measurement (BET BELLSORP MAX II & BELCAT-II, Microtrac BEL Corp, Japan)

6.2.4 Membrane performance

6.2.4.a Rejection of Cr (VI)

The permeability experiments were performed using the setup shown in Figure 6.1. The fabricated membranes were cut into proper size and mounted on the stainless steel membrane cell housing with the upper retaining plate and sealed with O-ring to avoid leakage. The filtration area (A) provided by the housing plate was 12.56 m^2. The membranes were initially compacted at 0.5 bar for 1 h to achieve a stable flux in the permeability set-up at the ambient temperature. The cell was provided with a glass vessel

for holding dichromate feed- the (chromium solution made from potassium dichromate (20,40,60,80 ppm, 500ml, pH 3,5,7,9) at the ambient temperature and was equipped with a magnetic stirrer The flux J_w (L/m^2h) was calculated by measuring the filtrate for 2 h and using equation 6.1

$$J_w = V_p/(A \times t) \quad (6.1)$$

where V_p is the mass of permeate (L), and t is the permeation time (h).

% Rejection of the fabricated membrane was calculated using equations 6.2

$$\% \text{ Rejection} = (1 - C_p/C_f)*100 \quad (6.2)$$

where C_f and C_p are the chromium concentrations in the feed and permeate,

The concentration of chromium was evaluated using method described in (APHA/AWWA/WEF, 1998). The detailed description is given section 6.2.4.c

6.2.4.b Photo-catalytic reduction of Cr (VI)

After 2 h, the concentrated chromium bearing retentate was collected in a 500 ml beaker having a PVDF/TiO_2 composite membrane piece and was subjected to photo-catalytic reduction under sunlight. 10 ml samples were collected at regular intervals and analyzed for Cr (VI). Reduction experiments were also conducted for all samples of retentate obtained under different operating conditions (pH, Cr(VI) concentration, pressure, particle loading and size). The % reduction was evaluated using equation 6.3

$$\% \text{ Reduction} = (1 - C_{rp}/C_{rf}) \times 100 \quad (6.3)$$

where C_{rf} and C_{rp} are the chromium concentration at t=0 min and t = t min.

6.2.4.c Analysis of Cr(VI) concentration

The Cr(VI) concentration was measured by the 1,5diphenylcarbazide method using a PC based double beam spectrophotometer **(**SYSTRONICS, PC Based Double Beam Spectrometer 2202, India**).** An aliquot (5 ml) containing Cr(VI) solution was diluted to 95 ml using DI water. 0.25 g of 1,5 biphenyl carbazide in 50 ml methanol was prepared from which 500 µL was added to 5 ml of prepared Cr solution and pH was maintained at 2 ± 0.5 using H_2SO_4 solution (APHA/AWWA/WEF, 1998). After 5 min, the absorbance of the purple color solution was measured by UV- spectrophotometer at 560 nm. Initially a calibration curve was prepared using standard dichromate solutions and then unknown solution concentration was evaluated using this standard plot.

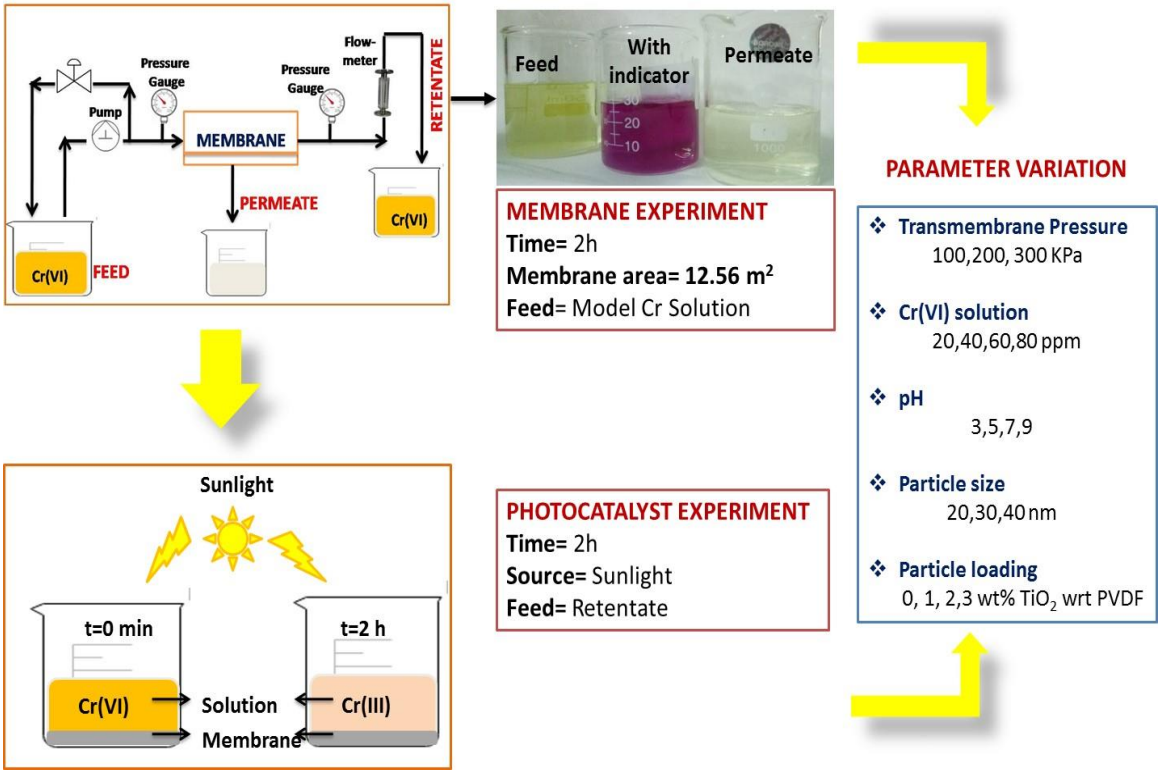

Figure 6.1: Schematic representation of setup for rejection of Cr(VI) using membrane and reduction of Cr(VI) using photo-catalyst

6.2.5. Response Surface Methodology and Optimization Analysis

6.2.5.a Experimental design using RSM

The response surface methodology (RSM) considers the interaction effects between the considered factors, which are ignored in conventional methods. It is the most widely used method to optimize and analyze the response of interacting variables and it reduces the number of experiments without affecting the interactive parameter (Goyal et al. 2011). A standard RSM design called central composite design (CCD) was employed to test the influence of independent variables (pH, chromium concentration, and particle loading) on the dependent variables: rejection and reduction of chromium from aqueous solution. The ranges of the above parameter were varied as: pH 5-8, Cr(VI) concentration 20, 40, 60, and 80mg/L and particle loading (0 wt%, 1 wt%, 2 wt% and 3 wt%). These three process variables were rigorously examined as these are primarily the main parameters affecting % rejection and % reduction and were optimized using the RSM Design Expert 8.0 software. The main goal, i.e., the maximum value of rejection and reduction, will determine the optimized values of the process variables and will indicate the performance of the TiO_2 enhanced PVDF polymer ultra-filtration process. The design comprised of 20 experimental trials including 6 centre points to maintain the accuracy obtained from software RSM of Design Expert 8.0 as shown in table 6.1. The number of experiments (M) was determined using equation 6.3 (Tan et al., 2008):

$$M = 2^m + 2m + m_c \qquad (6.3)$$

where m represents the number of independent variables (pH, Cr concentration and particle loading), m_c represents the number of replicate (centre point) thus the calculated number of experiments (M) is 20.

Table 6.1: CCD Experimental design of experiment matrix for Cr (VI) removal by PVDF/TiO_2 membrane

Runs	pH	Particle Loading	Concentration (mg/L)	Rejection (%)	Reduction (%)
1	3	0	20	6.01	12.5
2	3	3	20	88.03	80.25
3	3	0	80	4.98	11.37
4	3	3	80	85.4	76.98
5	8	0	20	5.9	11.31
6	8	3	20	81.02	72.1
7	8	0	80	5.4	11.24
8	8	3	80	79.1	70.25
9	5.5	0	50	5.54	11.5
10	5.5	3	50	86.54	76.98
11	5.5	1.5	20	90.14	85.25
12	5.5	1.5	80	87.03	70.2
13	3	1.5	50	89.99	75.5
14	8	1.5	50	87.48	71.99
15	5.5	1.5	50	88.32	74.98
16	5.5	1.5	50	88.32	74.98
17	5.5	1.5	50	88.32	74.98
18	5.5	1.5	50	88.32	74.98
19	5.5	1.5	50	88.32	74.98
20	5.5	1.5	50	88.32	74.98

To optimize the independent variables for the responses (% Rejection and % Reduction) obtained from experiments, the second-order polynomial equation incorporating

quadratic and interaction terms obtained from the CCD model was applied. The generalized mathematical form to represent the second-order equation is written as shown in equation (6.4).

$$R_y = \alpha_o + \sum_{i=1}^{m} \alpha_i X_i + \sum_{i=1}^{m} \alpha_{ii} X_i^2 + \sum_{i<j}^{m} \alpha_{ij} X_i X_j \quad (6.4)$$

where R_y denotes response, Xi and Xj are the coded values, α_o, α_i, α_{ii}, and α_{ij} are the regression, linear, quadratic, and interaction coefficients, respectively, m is the number of the design process variables. Analysis of Variance (ANOVA) was employed to validate the reliability of the equation generated using RSM. The statistical fitness of the CCD model was examined using different factors of ANOVA that include determination coefficient (R^2), adjusted determination of coefficient (R^2_{adj}), F value, p-value, and degree of freedom.

6.2.5.b Validation

Based on the optimum value as suggested by RSM, an experiment was performed at the given condition using an ultra-filtration setup. It consisted of a filtration cell of filtration area of 15.65 m^2. Initially, the membrane was pre-pressurized for half an hour at given pressure to achieve stable flux. Then 500 ml chromium solution at the suggested concentration and pH value was passed through the membrane. Chromium concentrations in retentate and permeate estimated using a spectrophotometer as described in Section 6.2.3.c. The retentate rich in the concentrated chromium (VI) was subjected to photo-catalytic reduction under sunlight. The retentate sample was poured into the beaker having the used washed membrane fixed at its bottom and the solution is continuously agitated with the help of agitator to avoid any concentration gradient. 2 ml samples were collected at regular intervals and analyzed for Cr (VI).

6.2.6 Stability and Reusability of Nanocomposite Membranes

The reusability of the membrane is also one of the vital factors for its successful application at large scale. The reusability test was carried out by running the experiments 5 times at the optimized operating conditions and using the same membrane material. After each run membrane sample was washed with Millipore water to remove residual from it and is again reused following the above described method. The membrane before and after experiment (UF and Photocatalytic Degradation experiment) was also analyzed using FTIR spectroscopic and BET surface area analyses to study the morphological changes.

6.2.7 Performance of membrane in real wastewater

At the suggested optimum conditions, the developed photo-catalytic membrane was used to treat a real wastewater using the same procedure as used for the model solution. Wastewater sample was collected from three different types of tannery industries located at the Industrial Area Site -2 Unnao, UP. The sample were collected from different units engaged in different leather production as Raw to finish, raw to wet blue and wet blue to finish and stored in 500 ml newly plastic bottles at ambient temperature (25°C)

Leather manufacturing is a three stage process namely: pre-tanning operation, tanning process and post tanning process including finishing. Raw to finish process includes all the three processing steps staring from processing of hides to wet blue leather (tanning of hides) formation to finished leather product. Raw to wet blue process includes pre-tanning operation, tanning process whereas wet blue to finish is engaged only in post tanning process. The samples collected from different units were passed through ultrafiltration setup as defined in Section 6.2.4.a. The permeate was collected at regular intervals and the rejected Cr(VI) solution was subjected for photocatalytic degradation according to the procedure defined in Section 6.2.4.b The chromium concentration was

measured using inductively coupled plasma-mass spectrometry (ICP-MS) (7800 ICP-MS mainframe, Agilent Technologies, US). Before ICP analysis, the sample were initially acid digested to remove other contaminants present in it. The chemical oxygen demand (COD) was evaluated using a COD Digester unit (UNIPHOS, Uniphos Envirotronic Pvt. Ltd, India)

6.3 RESULTS AND DISCUSSION

6.3.1 Mechanism for Cr(VI) removal from wastewater using bi-functional membrane

In an acidic solution at acidic pH Cr (VI) exist as $Cr_2O_7^{2-}$, CrO_4^{2-} and $HCrO^{4-}$ forms (Kazemi et al., 2018). The amphoteric nature of TiO_2 particles, due to protonation & deprotonation of hydroxyl groups on the surface exist as $Ti\text{-}OH_2^+$ in acidic environment as shown in equation (6.5)

$$(Ti - OH)_{surface} + H_3O^+ \leftrightarrow Ti\text{-}OH_2^+ + H_2O \quad (6.5)$$

Thus TiO_2 particles can adsorb the mentioned anions $Cr_2O_7^{2-}$, $CrO_4^{2-}$and $HCrO^{4-}$ due to the presence of $Ti\text{-}OH_2^+$. Thus it is the electrostatic interaction that is responsible for the rejection of Cr(VI) from wastewater when using TiO_2/PVDF membrane material during ultrafiltration. The same membrane when used as the photo-catalyst film reduces Cr(VI) in the retentate to Cr(III) through photo-catalytic process. It is established that on irradiation with sunlight the photons emitted are absorbed by TiO_2 and produce e^{-CB} and h^{+VB}as shown in figure 6.2 and equation (6.6-6.8)

$$TiO_2 + h\nu \rightarrow e^{-CB} + h^{+VB} \quad (6.6)$$

$$Cr_2O_7^{2-} + 14H^+ + 6e^{-CB} \rightarrow 2Cr^{3+} + 7H_2O \quad (6.7)$$

$$2H_2O + 4h^{+VB} \rightarrow O_2 + 4H^+ \quad (6.8)$$

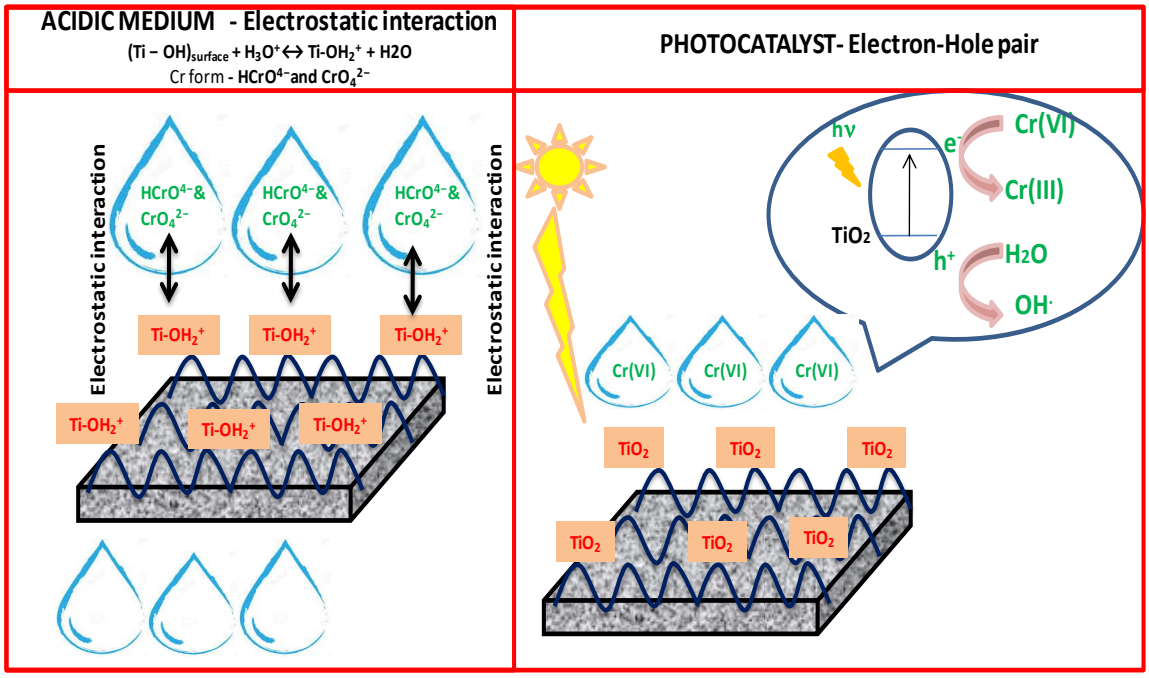

Figure 6.2: Schematic representation of the mechanism from Cr (VI) removal

6.3.2. UV spectra of Cr(VI) solution in feed, permeate, retentate and reduction side

The UV spectra of model Cr solution as shown in Figure 6.3(a) to 6.3(d) depict that the absorbance value of Cr(VI) in the permeate is very small compared to the absorbance of Cr(VI) in the feed as expected since membrane is not allowing the Cr(VI) ion to pass through it due to ionic interaction between membrane and Cr ion at acidic pH as a result the absorbance value in the permeate is small. Also the absorbance value of the retentate is higher than the feed which implies that Cr(VI) gets concentrated at the retentate side with time so its absorbance value is higher at feed side. Similarly it is seen from Figure 6.3 that after reduction process the absorbance value decreases with time in presence of nanocomposite membrane on exposure to light due to photo-catalytic reduction of Cr (VI).

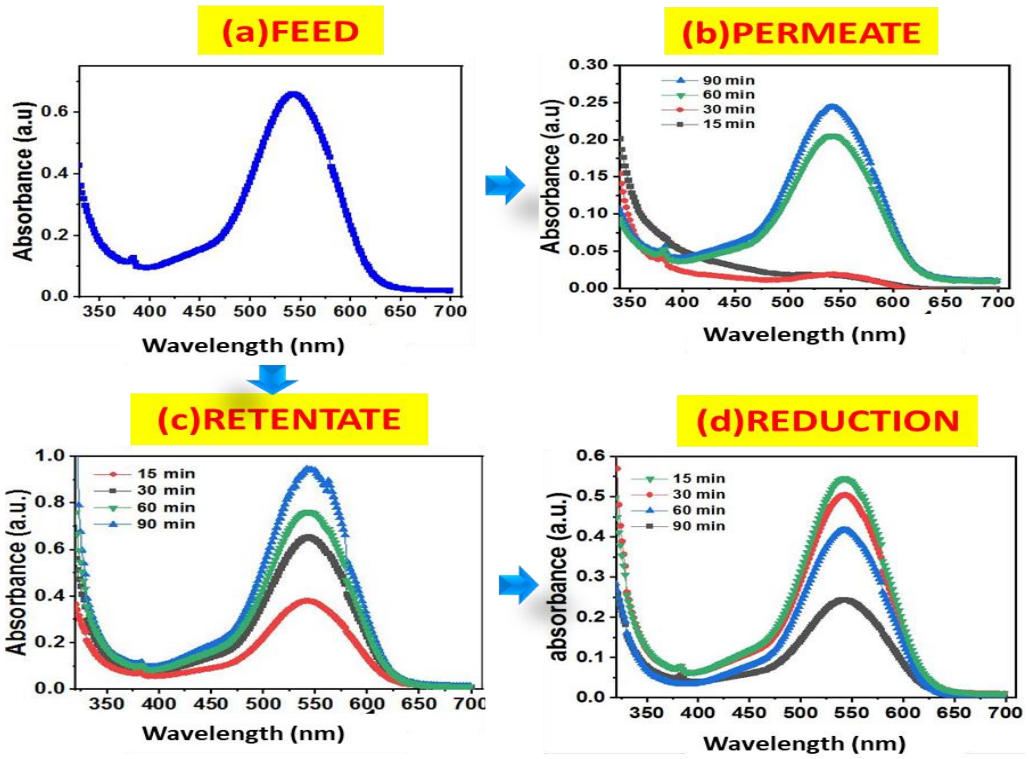

Figure 6.3: UV spectra of Cr(VI) solution (a) Feed (b) Permeate (c)Retentate (d) Reduction

6.3.3 Effect of Various Parameters

6.3.3.a Effect of TiO_2 Particle Loading on PVDF membrane

Effect of particle loading TiO_2 (wt%- 0%, 1%, 2%, 3%) with respect to PVDF polymer on the performance of nano-composite membrane is shown in Figure 6.4 at pH 5, trans-membrane pressure (ΔP) 300 KPa, [Cr (VI)] 20 ppm and particle size 20 nm. Figure 6.4(a) depicts that the flux increases from 50 to 280 L/m^2h as the particle loading increases from 0 (PM1) to 2 wt% (PM3). This result is expected because of the presence of hydrophilic TiO_2 NPs. As already mentioned in Chapter 3 addition of particles increases the porosity and pore size of the membrane and reduces the contact angle. Thus indirectly

implying that the increased porosity will increase the water flux. Also the hydrophilic characteristic of the particles will attract more molecule of water to pass through thus increasing the flux. However at the maximum loading of 3 wt% (PM4) the flux declines due to aggregation of particle at high concentration leading to a reduction in the porosity and pore size of the membrane.

A similar trend was also observed for the % rejection as shown in Figure 6.4 (b) where the lowest % rejection (<10%) was obtained for the PM1 membrane with no particle loading and the highest value (>90%) was obtained in case of PM3 membrane. The increased concentration of particles increases the number of active site on the membrane thereby inducing an increased electrostatic interaction between the membrane surface and Cr (VI) ions. This increased interaction will not allow the ions to pass through the membrane rather they will be rejected on the retentate side therefore value of rejection will increase with increase in the particle loading. In case of PM4 membranes the particle aggregation reduces the number of active sites therefore the electrostatic interaction between membrane and Cr(VI) ions will be less compared to PM3 membrane and the rejection will decrease, however, it is still higher

The increase in concentration of NPs from 0 to 2 wt% increases the generation of e^{-CB} and h^{+VB} when exposed to sunlight. More the number of e^{-CB} and h^{+VB} more will be the number of Cr (VI) ions reduced to Cr (III) ion as a result %reduction increases with increase in the particle concentration (Figure 6.4 (c)). Opposite trend was observed for PM4 membrane where agglomeration of particles results in a decreases in the active surface area available for the photon to generate more number of e^{-CB} and h^{+VB}. Thereby less number of Cr (VI) ions will be reduced to Cr(III) under otherwise identical conditions. Thus the

membrane PM3 with 0.2 wt% of TiO_2 loading was selected as the best membrane at which excellent results for flux, % rejection and % reduction were obtained. Hence this membrane will be used in further experiments.

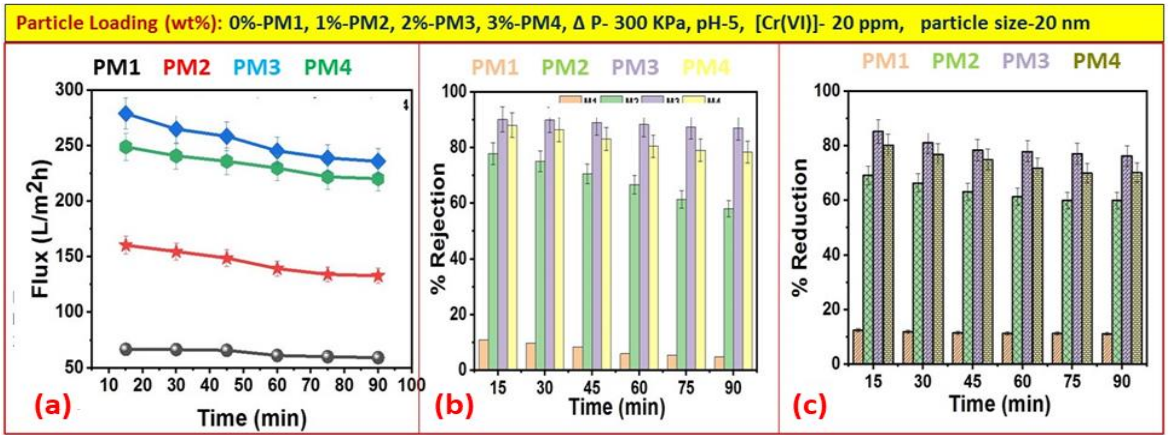

Figure 6.4: Effect of NPs loading: (a)Variation of Flux, (b)% rejection and (c)% reduction with time

6.3.3.b Effect of Particle size

Effect of particle size on the performance of nano-composite membrane is shown in Figure 6.5 for particle loading of 2 wt% at pH 5, trans-membrane pressure (ΔP) 300 KPa, and [Cr (VI)] 20 ppm. Figure 6.5(a) shows that the flux decreases from 285 to 265 L/m^2h approximately as the particle size increases from 20 to 40 nm which is attributed to pore blockage of the membrane by the bigger size particle. The impact of pore blockage is more than the hydrophilicity of the membrane. The pore blockage will also results in decrease in number of pores per unit membrane area, so porosity will decline due to which flux also decline.

The Cr (VI) rejection was found to decrease with increase in particle size from 20 to 30 nm as shown in Figure 6.5 (b). The increased particle size will reduce the active

surface area available for the ionic interaction to take place between the membrane and Cr ions at acidic pH. Decreased interaction will ultimately affect the rejection performance of the membrane.

Similar results were also observed for % reduction (Figure 6.5(c)). As mentioned above increased particle size reduces active surface area available to generate large number of e^{-CB} and h^{+VB} to reduce Cr (VI) to Cr(III) form. Thus it is seen that the large particle size is not preferable for good performance of the nano-composite membrane. Thus a particle loading of 2 wt%, and particles of size 20 nm was selected as the best combination for excellent performance keeping all other parameter constant.

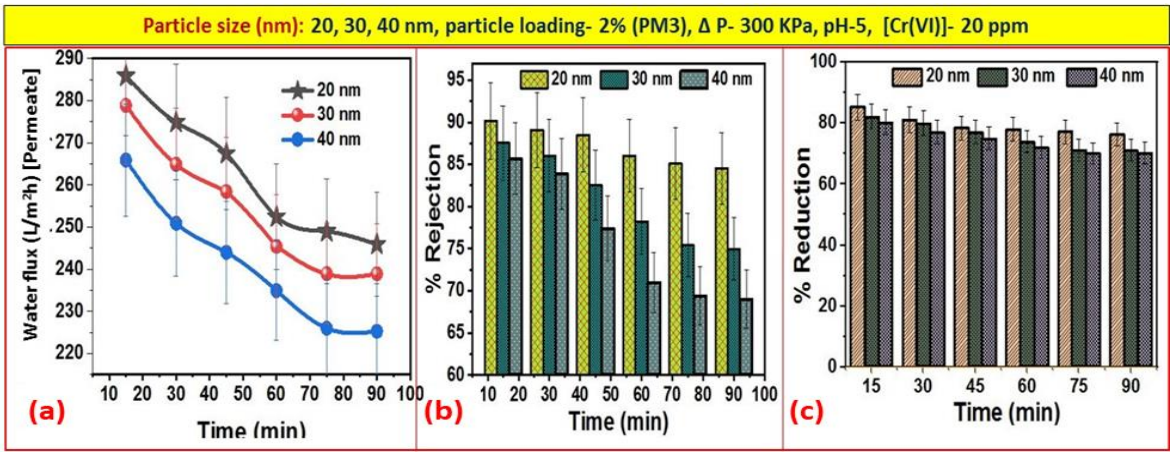

Figure 6.5: Effect of particle size: (a)Variation of Flux, (b)%rejection and (c)% reduction with time

6.3.3.c Effect of pH

The pH is considered as one of the crucial parameters affecting the membrane performance in Cr (VI) removal from the feed solution. Figure 6.6 show the effect of pH on flux, % rejection and % reduction. The figure depicts excellent performance was achieved

that at the acidic pH compared to the basic. Figure 6.6(a) shows that the flux changed from 100 to 280 L/m^2h when the pH was changed from 9 to 3. As already explained in Section 6.4.1 that at the acidic pH Cr(VI) exists in anionic forms whereas TiO_2 exists as Ti-OH_2^+ in polymer matrix, as a result the electrostatic interaction between Cr(VI) ions and membrane surface is more compared to that at basic pH due to which it will not allow Cr(VI) ions to pass through it. The water molecules, however, will pass through resulting in an increase in the water flux on the permeate side with decrease in pH. Further, the values of water flux at pH 3 and 5 are nearly similar. Since the pH of chromium bearing wastewater from tanneries lies in the range of 5 to 6 so pH 5 has been selected as the best pH for achieving high value of water flux on the permeate side under practical situations.

From Figure 6.6 (b) it is seen that the %rejection of Cr (VI) ions is >90% at pH 3 and 5, compared to 7 and 9. It is attributed to the formation of Ti-OH_2^+ at acidic pH where Cr (VI) exists as $Cr_2O_7^{2-}$, $CrO_4^{2-}$and $HCrO^{4-}$ ions as a result the interactions with membrane will be more at lower pH which is not the case at basic pH. Under alkaline conditions pH>7, Cr (VI) exists as H_2CrO_4 therefore the interaction between the membrane and Cr ions in the feed solution is minimal as a result the rejection is less (<60%) as observed at pH 9. Hence acidic pH is to be preferred over basic pH for Cr (VI) ion removal from the feed solution.

Figure 6.6(c) depicts the variation of % reduction with time at different pH (3, 5, 7 and 9). It is seen here again that acidic condition favours the photo-catalytic reduction of Cr (VI) ion to Cr (III) ion. Under acidic conditions, positive charge on NPs will adsorb Cr (VI) ions strongly due to opposite charge interaction. It was also reported by Hudaya et al. (2013) that at low value of pH, potential increases and is more positive than the conduction

band of TiO_2 NPs. Thus at low pH reduction of Cr (VI) ion is thermodynamically favourable as a result % removal is more at acidic pH

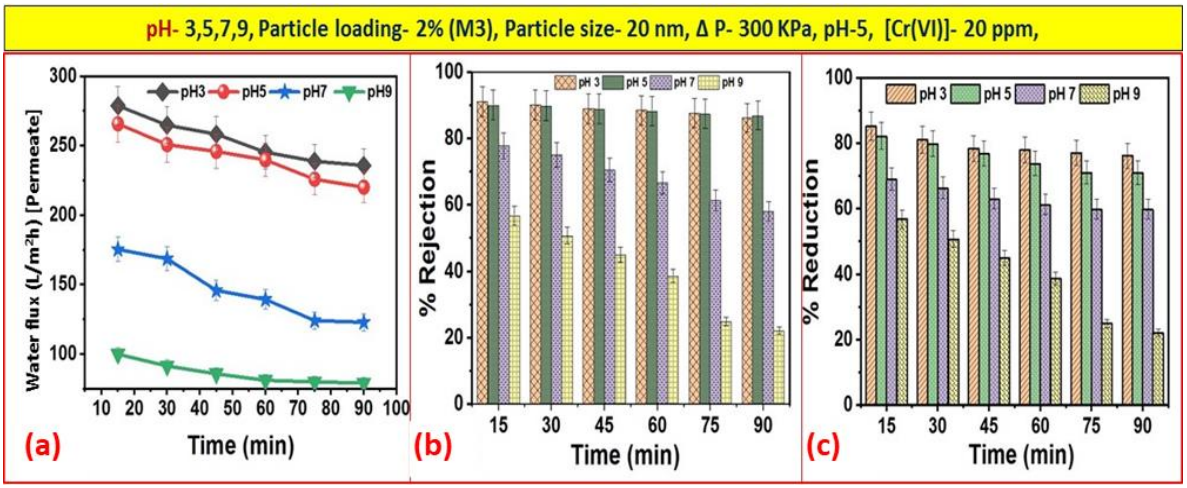

Figure 6.6:Effect of pH (a)Variation of Flux, (b)%rejection and (c)% reduction with time

6.3.3.d Effect of Cr (VI) concentration

The concentration of Cr is another important parameter affecting the membrane performance in Cr (VI) removal from the feed solution. Figure 6.7 (a) to 6.7 (c) show the effect of concentration on the flux, % rejection and % reduction, respectively. These figures depict that concentration shows an inverse relation with flux % rejection and % reduction. The flux decreased from 280 to 170 L/m^2h when the Cr (VI) concentration increased from 20 to 80 ppm (Figure 6.7 (a)). It is due to the fact that at increased concentration (at acidic pH, 2 wt % TiO_2 loading) results in excess Cr(VI) ions in the feed solution will inhibit passage of water molecules through the membrane and decrease the permeate side flux.

Figure 6.7(b) shows the effect of feed concentration on the variation of %rejection with time. It is seen that the %rejection has decreased from 90 to 80% when the Cr(VI) concentration changed from 20 to 80 ppm. It is due to fact that at acidic pH, the membrane incorporated with TiO_2 gets saturated with Cr(VI) ions and after that the Cr(VI) ions do not show the ionic interaction with membrane due to unavailability of $Ti\text{-}OH_2^+$ charge on the membrane. Thus it will affect the rejection efficiency of the membrane.

Figure 6.7(c) shows an inverse trend between % reduction and Cr(VI) concentration. In case of photo-catalyst reduction process, the increased concentration will interfere with the light reaching the photoctalyst surface due to increased absorbance capacity at high concentration (the screening effect), thereby reducing the degree of reduction (Qamar et al. 2011). These results also indicate that with all other conditions remaining unchanged the PVDF/TiO_2 membrane with 2 wt% TiO_2 loading of size 20 nm gives maximum %reduction at pH 5 and Cr(VI) concentration of 50 ppm.

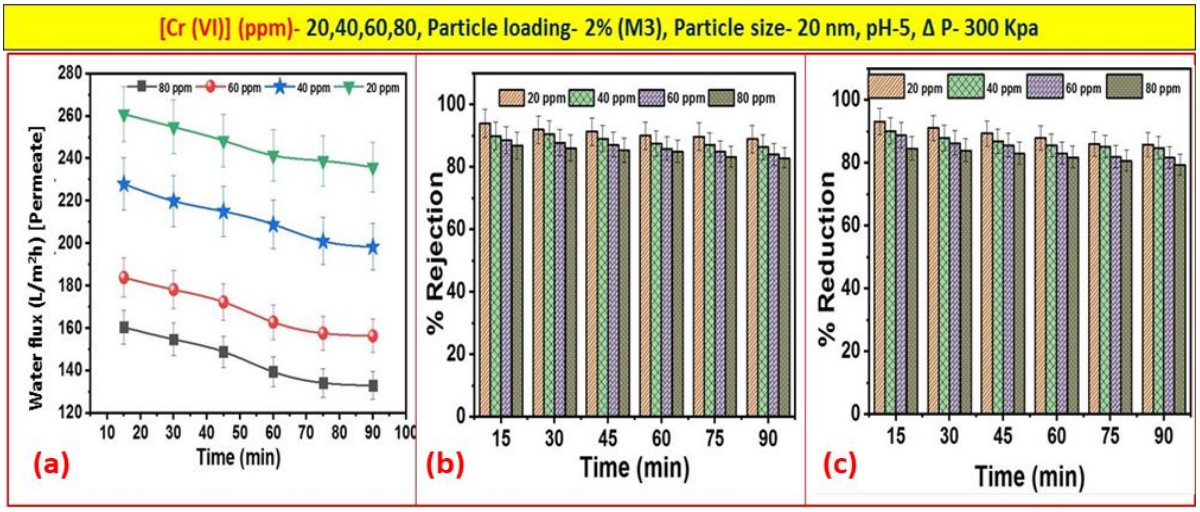

Figure 6.7: Effect of [Cr(VI)]: (a) Variation of Flux, (b) %rejection and (c)% reduction with time

6.4.3.e Effect of Trans-membrane Pressure

Trans-membrane pressure is the pressure gradient between permeate and feed sides. More the gradient more will be the solvent transfer hence more will be the value of flux. Figure 6.8 show the effect of trans-membrane pressure on variation of flux and %rejection, respectively. -The permeate flux showed a linear relation with increasing trans-membrane pressure as expected (Figure 6.8 (1)). The increase in %rejection was also observed to increase on increasing the pressure (Figure 6.8 (2)) due to increase in solvent convective transport, similar trend was also reported by Riaz et al. (2016). Thus at the loading of 2 wt% particles of 20 nm size at pH 5 and [Cr] concentration of 20 ppm, 300 KPa was taken as optimum pressure at which excellent result was obtained.

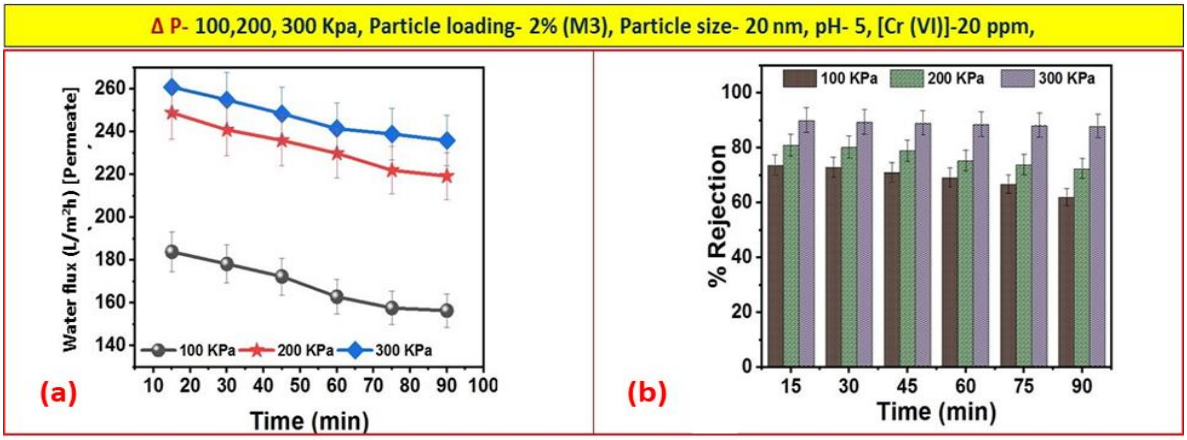

Figure 6.8: Effect of transmembrane pressure: (1) Variation of flux, (2) % Rejection with time

6.3.4 RSM and ANOVA analysis

6.3.4.a Data adequacy check of the model

The set of experiments as suggested by RSM were performed and the experimentally obtained data were analysed using ANOVA analysis. Figure 6.9(a) and 6.9(b) depict the plots of actual versus predicted responses for % Rejection and % Reduction, respectively

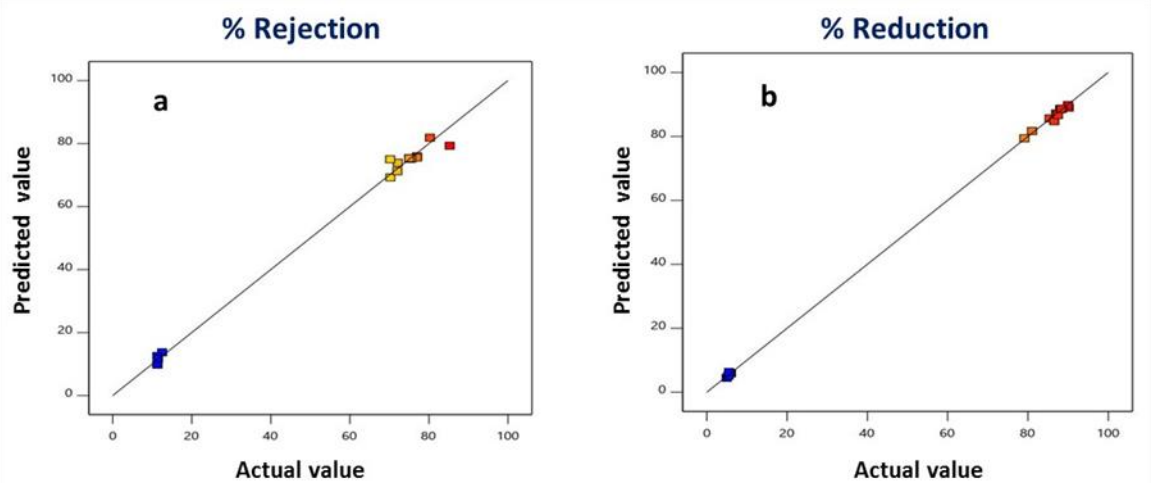

Figure 6.9: Actual vs. predicted plot of the model: (a) % Rejection (b) % Reduction

Here the actual values were determined experimentally, and predicted values were calculated by the RSM model. These plots indicate that the model is adequate and ensures the acceptability of the predicted values because almost all the points in both the plots lie on the diagonal line (Lu et al., 2009). Model reliability was further assured in terms of R^2. Here the high value of R^2 and adjusted R^2> Predicted R^2 in case of % rejection is 0.9994>0.9980, and for % reduction, it is 0.9905>0.9617, these confirm that the experimental results fit well with the predicted values.

6.3.4.b Effect of independent (process) variables on % Rejection

The quadratic order has been suggested for regression analysis without any transformation, and the RSM equation in terms of the actual factor is shown in the following equation 6.9

% Rejection = 88.6458 + 39.226 * A + -0.919 * B + -1.551 * C + -0.3775 * AB + -1.7025 * AC + 0.155 * BC + -43.0945 * A^2 + -0.549545 * B^2 + -0.399545 * C^2 (6.9)

The fitted model includes each contributing factor for a response. The adequacy of the second-order equation was analyzed using Fisher's statistical test (*F-value)*. *F-value* is defined as the ratio of (the mean square $_{\text{regression}}$) to (the mean square $_{\text{residual or real error}}$). The suitability of the model is well defined as a probability value (p-value) < 0.05 with a high F-value. The value of $p < 0.0001$ and F-value of 3709.67 as shown in Table 6.2 imply that the model is statistically significant and is well suited to the experiments. It is not necessary to have all term significant in regression analysis. If p-values of regression are less than 0.0500 affirmed that terms are significant, and here as shown in Table 6.2 linear term namely, pH, particle loading, concentration, and quadratic term (particle loading)^2 are significant model terms. Moreover, the model significance was further reinforced by the "Adeq Precision" ratio, which was found to be 32.147 and indicates an adequate signal as a ratio above 4 is desirable, hence can be effectively used to navigate design space.

Table 6.2: ANOVA summary for % rejection from CCD model

Source	Sum of Squares	D_f	Mean Square	F-value	p-value	
Model	24978.54	9	2775.39	3709.67	< 0.0001	Significant
A	15386.79	1	15386.79	20566.40	< 0.0001	

B	8.45	1	8.45	11.29	0.0072
C	24.06	1	24.06	32.15	0.0002
AB	1.14	1	1.14	1.52	0.2453
AC	23.19	1	23.19	30.99	0.0002
BC	0.1922	1	0.1922	0.2569	0.6232
A^2	5107.13	1	5107.13	6826.33	< 0.0001
B^2	0.8305	1	0.8305	1.11	0.3169
C^2	0.4390	1	0.4390	0.5868	0.4614
Residual	7.48	10	0.7482		
Lack of Fit	7.48	5	1.50		
Pure Error	0.0000	5	0.0000		
Cor Total	24986.02	19			

The regression equation (6.9) generates graphical response surfaces. This response plot helps in determining the individual and combined effects of three independent variable independent variables. Based on ANOVA analysis it was observed that pH is a more significant parameter followed by the concentration, and particle loading on % rejection of Cr (VI). Figure 6.10 shows the 3-D plot of response as a function of independent variables. Figures 6.10(a & b) depict lesser % rejection at lower particle loading and similar results were also obtained by Gasemloo et al. (2019) and Zang et al. (2020). At low particle loading, number of active site available in the form of $TiOH^+$ are smaller therefore lesser number of Cr (VI) ions will be rejected by the membrane. A trend opposite to that of particle loading was observed on increasing the pH as shown in Figures 6.10 (b & c). It is due to fact that at low pH value Cr(VI) exist in anionic form ($HCrO^-_4$) and positive charge

is induced on the membrane surface due to the presence of TiO_2 NPs; as a result strong electrostatic interaction leads to increased Cr removal. This implies significant impact of pH on % rejection. Trend similar to pH was observed on increasing the Cr (VI) concentration as shown in Figures 6.10 (a & c). The increased concentration at acidic pH generates an excess anionic charge on the membrane surface, thus creates a negative impact on the separation efficiency of membrane. These results conclude that there is considerable interaction of independent parameters for optimization of % Rejection and also highlights that pH, particle loading, and Cr (VI) concentration are important factors affecting the membrane performance.

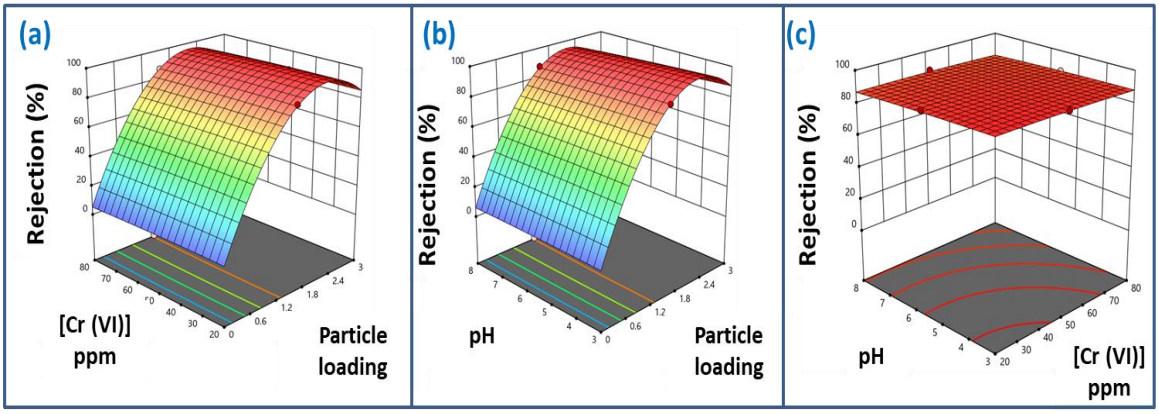

Figure 6.10: 3D dimensional response surface and contour plots of % Rejection showing the effect of (a) Particle loading and Cr(VI) concentration (b) pH and particle loading; (c) pH and Cr (VI) concentration

6.3.4.c Effects of independent variables on % Reduction

The statistical equation obtained for the %reduction using RSM is shown as equation 10

% Reduction = 75.3436 + 31.864 * A + -2.137 * B + -1.971 * C + -0.49 * AB + -1.695 * AC + 0.31 * BC + -31.6491 * A^2 + 1.83591 * B^2 + -2.14409 * C^2 (6.10)

Here also p-value <0.0001 and F of 220.43 (Table 6.3) from ANOVA analysis affirms that the model is significant. It is also observed that p value is <0.05 for linear terms (pH, particle loading and Cr concentration) and quadratic term (particle loading^2) signifies remarkable impact of these independent variables on % reduction.

Table 6.3: ANOVA analysis for % reduction from CCD model

Source	Sum of Squares	Df	Mean Square	F-value	p-value	
Model	15346.40	9	1705.16	220.43	< 0.0001	Significant
A	10153.14	1	10153.14	1312.54	< 0.0001	
B	45.67	1	45.67	5.90	0.0355	
C	38.85	1	38.85	5.02	0.0489	
AB	1.92	1	1.92	0.2483	0.6290	
AC	22.98	1	22.98	2.97	0.1155	
BC	0.7688	1	0.7688	0.0994	0.7590	
A²	2754.58	1	2754.58	356.10	< 0.0001	
B²	9.27	1	9.27	1.20	0.2993	
C²	12.64	1	12.64	1.63	0.2300	
Residual	77.35	10	7.74			
Lack of Fit	77.35	5	15.47			
Pure Error	0.0000	5	0.0000			
Cor Total	15423.76	19				

Response 3-D plots for % reduction showing the interaction between independent and dependent variables are shown in Figure 6.11. Figures 6.11 (a & b) depict that particle loading plays a crucial role during photo-catalytic reduction process this is attributed to the fact that at as the particle amount within the polymer matrix increases more generation of

electron and hole pair will be there to accelerate the reduction of Cr (VI) to non-toxic form Cr (III). Therefore direct impact of particle loading on the value of % reduction is observed. From Figures 6.11 (b & c) it is observed that at acidic pH the performance is excellent compared to basic pH this is due to fact that variation in pH will influence the surface charge directly affecting the photo-reduction process (Mohamed et al., 2016). They obtained a similar trend for % Rejection. These results confirm that % reduction will be higher at acidic pH. Figures 6.11 (a & c) show the effect of Cr(VI) concentration on % reduction. It was concluded that with an increase in concentration at constant pH photo-reduction efficiency decreases. This is attributed to the fact that increased concentration will interfere with the light reaching the photo-catalyst surface due to increased absorbance capacity at high concentration, thereby reducing the degree of reduction (Qamar et al. 2011). It can be thus concluded that pH, particle loading and concentration significantly affect both the responses (% rejection and % reduction).

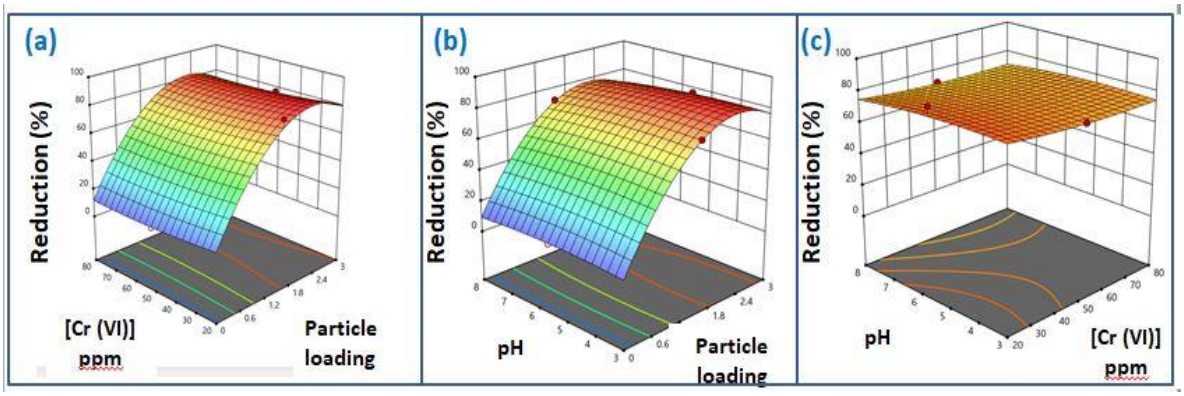

Figure 6.11: 3D dimensional response surface and contour plots of % reduction showing the effect of (a) Particle loading and Cr (VI) concentration, (b) pH and particle loading and (c) pH and Cr (VI) concentration.

6.3.4.d Optimization and validation of optimized results

After the establishment of the quadratic equation relating the dependent variable with the independent variable, it is checked further for optimization. The main objective of the experimental design and optimization is to determine the optimum values of the parameter at which maxima or minima of the response output could be achieved. In this study the desired goal for the two responses is set as "maximum," while for process variable, the desired goal was marked as "range". The optimum results obtained from numerical optimization using CCD model is shown in Table 6.4. Under the given optimum conditions, an experiment was performed to verify and validate the results. The experimental result obtained was consistent with the results obtained from RSM and hence validated the findings of response surface optimization, and the percentage error is almost negligible.

Table 6.4: Predicted and Experimental (Actual) value at optimized condition

	Loading (wt%)	**[Cr (VI)] (ppm)**	**pH**	**Rejection (%)**	**Reduction (%)**
Predicted	2.407	25.13	5.2	92.45	87.42
Observed	2.41	25	5.0	91.58	87.02

6.3.5 Reusability and Stability

At the given optimised conditions to test the reusability of PVDF/TiO_2 membrane the experiment was run repeatedly for 5 times, and the results are shown in Figure 6.12, 6.13 & 6.14. No significant loss in the value of rejection and reduction could be observed after five runs (Figure 6.12 (a)) which implies that synthesized PVDF/TiO_2 membrane retains its reusable capacity. Particle stability within the polymer matrix is another

important point. There may be a possibility that particles may leach out during application and can affect the hydrophilicity. The measurement of the contact angle may act as a stability indicator (Arif et al., 2019). Figure 6.12 (b) depicts the contact angle of the cleaned membrane after Cr (VI) removal. It is seen that no drastic difference in value for fresh and used membranes are observed, which proves excellent stability of synthesized TiO_2 NPs within the PVDF polymer.

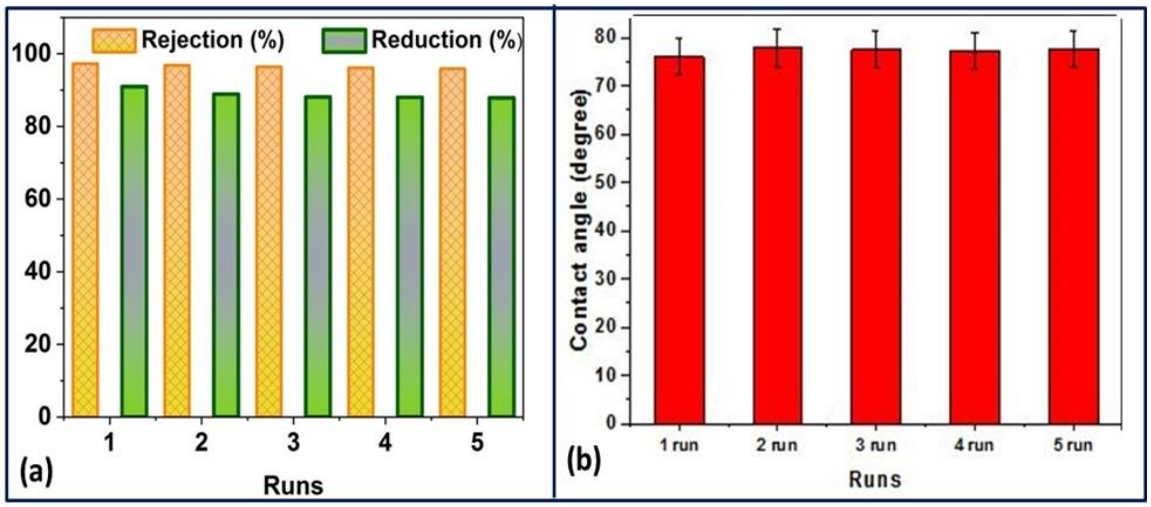

Figure 6.12: (a) Reusability of PVDF/TiO_2 membrane for Cr (VI) removal (b) Contact Angle value of the membrane after each run

Figure 6.13 shows the FTIR spectra of the composite membrane at different conditions during the experiment. It is observed that peaks obtained for cleaned membrane after separation and photo-catalyst application are similar to the fresh membrane (original membrane). Peaks at wavelength 3748, 1658 corresponds to the hydroxyl group from TiO_2 and peak at 640 cm^{-1} corresponds to Ti-O-Ti bonds (Bhute et al., 2017). It signifies that no morphological changes are observed; hence the membrane retains its property even after using it as membrane and photo-catalyst film. After completion of the separation process, peaks are either diminish or vanished, which signifies that these peaks play a great role for

separation because, as already mentioned it is the ionic interaction that is responsible for the separation of Cr(VI) from wastewater.

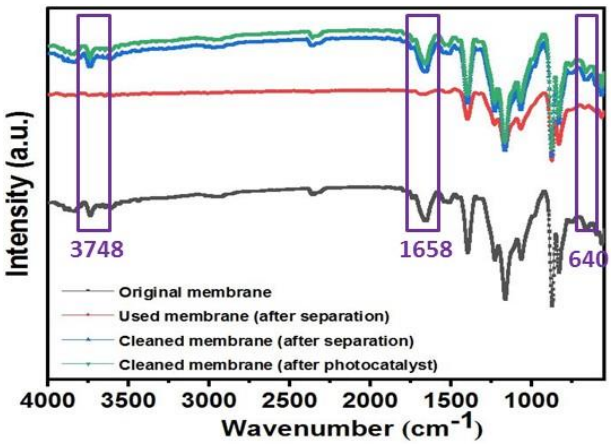

Figure 6.13: FTIR spectra of membrane before and after treatment

The results of BET (Brunauer, Emmett and Teller) analysis of composite film before and after Cr(VI) removal is shown in Figure 6.14. The estimated BET surface area before and after Cr(VI) removal using the BET equation was 383.5 and 366.7 m^2/g respectively. Here also decline in surface area is not that significant which implies that PVDF/TiO_2 membrane is having excellent recyclability without much reduction in its efficiency.

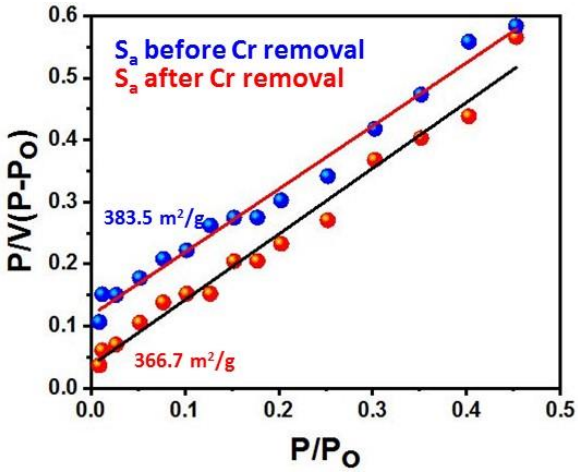

Figure 6.14: BET surface area of membrane before and after Cr removal

6.3.6 Performance of Membrane using real waste water

Lastly, the performance of the synthesized membrane was tested using real tannery wastewater collected for different tanneries. The results obtained are shown in Figure 6.15. In all three type of production process value of TSS, Cr(VI) and COD in permeate is minimal which indicates excellent separation efficiency even though the Cr(VI) concentration in collected sample (feed side) ranges between 75 mg/L to 18 mg/L from type 1 to type 3 units at acidic pH . Rejection Efficiency was approximately observed to be 87% for Type 1, 90% for Type 2 and 91.5% for Type 3 whereas the reduction % in all three cases was observed to be greater than 85% which is comparable to results obtained using the model chromium solution. Thus it can be said that green synthesized TiO_2 nano-particle embedded in PVDF polymer provides can be used to treat wastewater in a cost-effective way using the cost effective ultra-filtration process. These results also implies particle synthesized using green solvent provides good scope to use as filler to enhance the property of PVDF polymer.

Figure 6.15 also depicts that pH of the solution at permeate side and after photocatalytic reduction process in all three cases is nearly neutral which again add advantage because now the treated water can be reused again without adding any chemical to neutralize the pH of treated water. The value of TSS, Cr(VI) and COD at retentate side is higher than the feed side also which is expected because of increased concentration of Cr(VI) and other contaminant due to excellent rejection property of membrane

TYPE OF PRODUCTION		* F= Feed, P= Permeate, R= retentate, D= After Photocatalytic Reduction
TYPE 1	RAW TO FINISH 	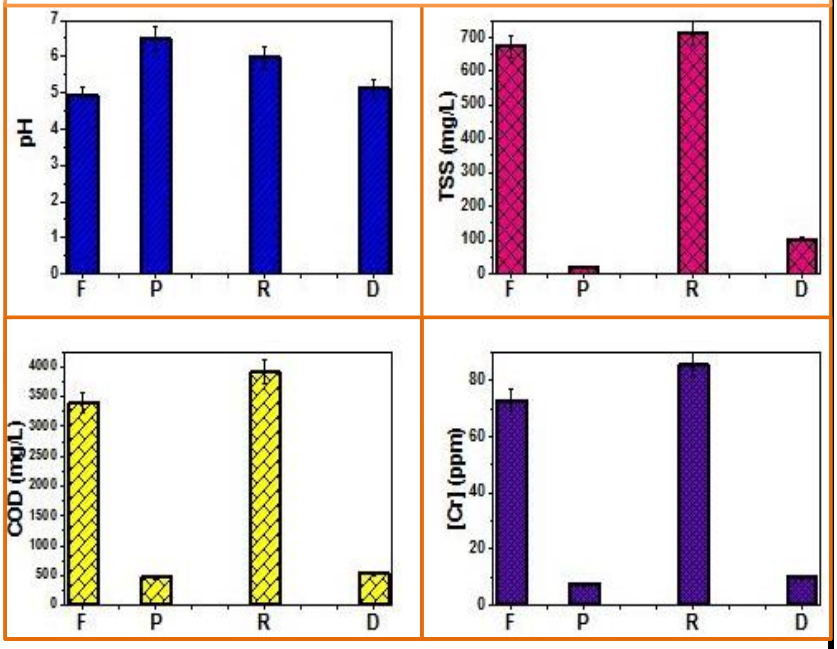
TYPE 2	RAW TO WET BLUE 	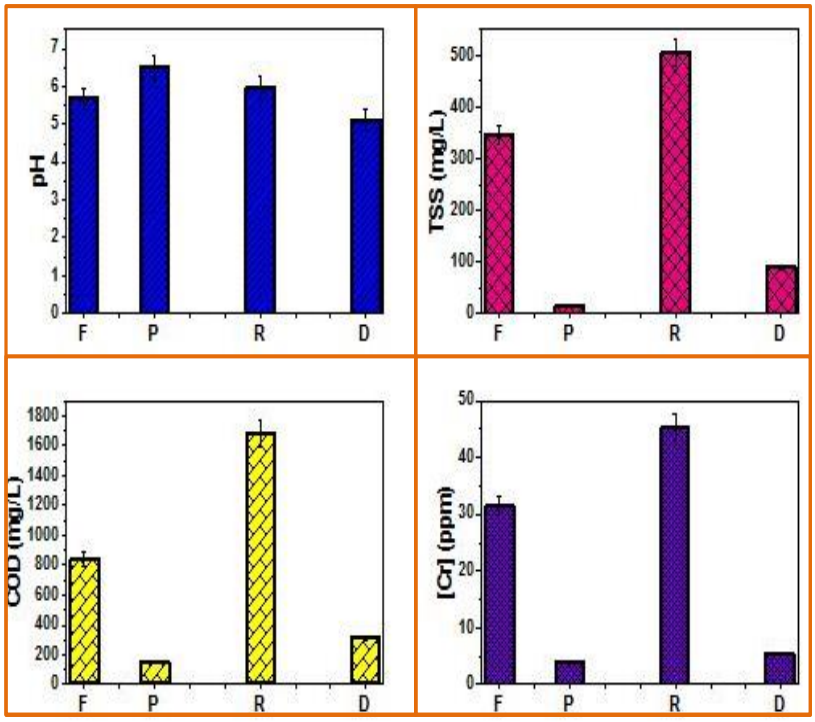

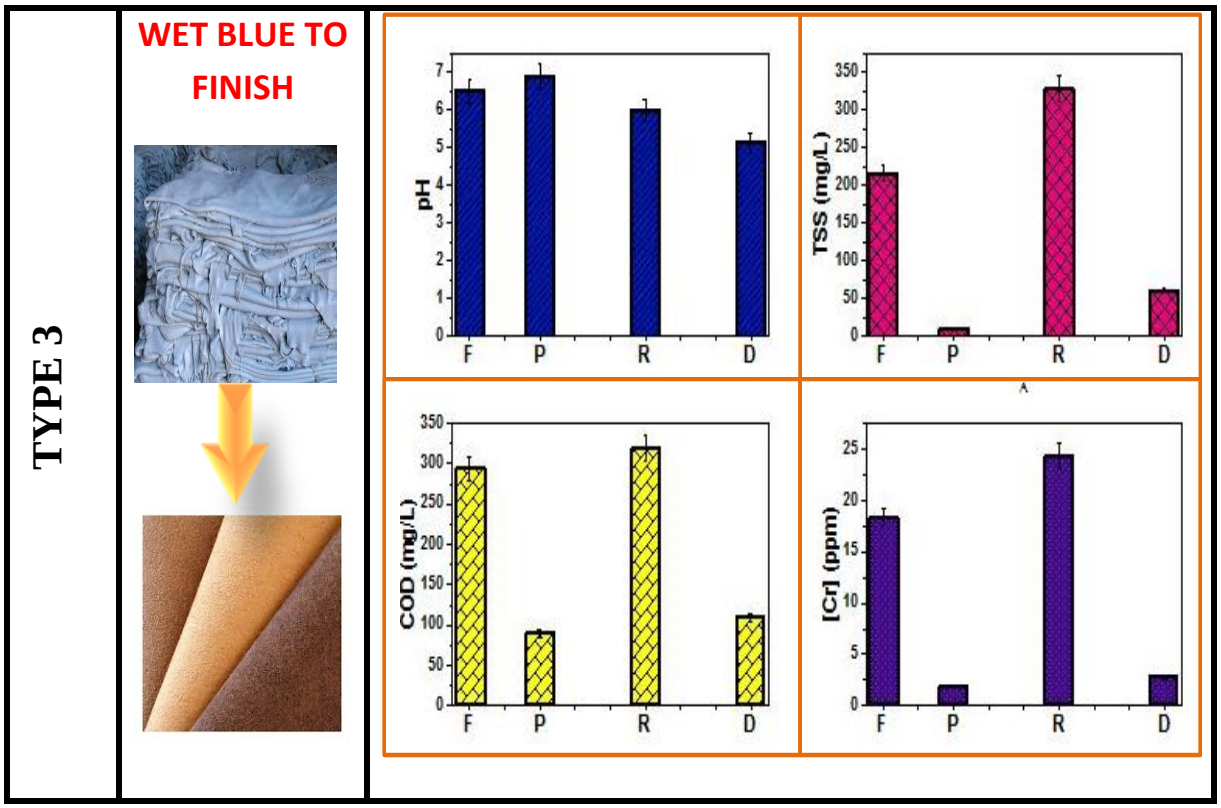

Figure 6.15: Graph of pH, TSS, COD, and Cr for wastewater before and after treatment for 3 different types of tannery industry

A comparative study is also carried to compare the efficiency reported in this work with other published literature, as shown in Table 6.5. It is concluded from the table that either expensive technique is required to treat real wastewater to achieve rejection >90%, or in other cases, if separation efficiency is > 90%, it is only reported for model Cr solution. However, in this study, both separation efficiency and % reduction is quite high and applicable for both model and real solution using cost-effective ultra-filtration process.

Table 6.5: Comparative study of present study with other published literature

Process	**Synthesis/ Commercial**	**% Removal**	**Reference**
Anaerobic nano zero-valent iron granules	Synthesized	**Model Cr solution** 88 ± 1.56% rejection	Venkatagiri et. al., 2019
Membrane bioreactor and reverse osmosis treatment	Synthesized	**Real waste water** 97% rejection	Scholz et al., 2005
Nanofiltration membrane	Synthesized	**Real wastewater** 60-80% rejection	Mohammad et al., 2019
Conductive Ultrafiltration	Synthesized	**Model Cr solution** 72.4% rejection	Liu et al., 2019
Amine-impregnated TiO_2nanoparticles modified cellulose acetate membranes	Synthesized	**Model Cr solution** 72.4% rejection	AlebelGebru and Das, 2018
Polyamide skin over a polysulphone support - nanofiltration. (NF) and Polyamide - reverse osmosis (RO)	Commercial	**Real wastewater:** Approx 97% Cr removal	Das et al., 2006
PVDF/TiO_2 ultrafiltration membrane	Synthesized bi-functional membrane	**Model Cr solution** 7.2 % rejection and 90.98% reduction **Real waste water:** >90 % rejection and >88% reduction	This work

6.4 CONCLUSION

The present investigation established the efficacy of low cost synthesized PVDF/TiO_2 membrane using green synthesized TiO_2 NPs for removal of Cr(VI) from wastewater. Different operating parameters (particle loading, particle size, solution pH, Cr(VI) concentration and trans-membrane pressure) were varied to study their effect on % removal and %reduction. An attempt has also been made to apply RSM for the optimization of the performance of bi-functional ultra-filtration membrane for Cr(VI) removal from aqueous solutions and lastly at optimized condition, results are validated using both model and real wastewater.

The results suggested that incorporation of 2 wt% of TiO_2 nano-particles particles of size 20 nm in the PVDF membrane matrix results in a membrane having best performance at 5 pH and 300 kPa for the efficient treatment of 20 ppm Cr(VI). The CCD model proves to be an effective statistical tool for optimization. Results obtained using CCD indicate that the maximum theoretical values of % rejection and % reduction at optimum condition are 92.45% and 84.72% respectively and equal to the experimental results under same conditions. It has been observed that interaction of pH and concentration is more significant in case of % rejection and % reduction, however pressure is only significant parameter in case of % rejection. For the real waste water it gave approximately 91.58 % rejection and 87.02% reduction which implies that a low cost photo-catalytic ultra-filtration membrane has been successfully developed.

Membrane stability and reusability capability was also evaluated by running the experiment 5 times using same used membrane and it was concluded that no morphological changes was observed before and after the experiment confirmed from BET and FTIR

analysis also the rejection and reduction % values remains unchanged signifies good reusable strength.

6.5 REFERENCES

AlebelGebru, K, Das, C, Removal of chromium (VI) ions from aqueous solutions using amine-impregnated TiO_2 nanoparticles modified cellulose acetate membranes. Chemosphere 191(2018)673-684

Arif, Z, Sethy, N K, Kumari, L, Mishra, P K, Verma, B, Antifouling Behaviour of PVDF/TiO_2 Composite Membrane: A Quantitative and Qualitative Assessment. Iranian Polymer Journal 28(2019)301–312.

Arif, Z, Sethy, N K, Kumari, L, Mishra, P K, Verma, B, Green synthesis of TiO_2 nanoparticles using *Cajanus cajan* extract and their use in controlling the fouling of ultrafiltration PVDF membranes. Korean Journal of Chemical Engineering 36(7)(2019)1148-1156

Barakat, MA, Schmidt, E, Polymer-enhanced ultrafiltration process for heavy metals removal from industrial wastewater. Desalination 256(2010)90–93

Bhute, MV, Mahant, YP, Kondawar, SB, Titanium dioxide/poly(vinylidene fluoride) hybrid polymer composite nanofibre as potential separator for lithium ion battery. Journal of Material Nano Science, 4(1) (2017) 6-12

Burakov,A E, Galunin,E V, Burakova, I V, Kucherova,A E, Agarwal, S Tkachev, A G et al., Adsorption of heavy metals on conventional and nanostructured materials for wastewater treatment purposes: A review, Ecotoxicology Environmental Safety 148(2018) 702–712.

Choi, H, Stathatos, E, Dionysiou, D D, Sol–gel preparation of mesoporous photocatalytic TiO_2 films and TiO_2/Al_2O_3 composite membranes for environmental applications. Applied Catalysis B: Environmental 63(2006) 60-67.

Choudhury PR, Majumdar S, Sahoo GC, Saha S, Mondal P, High pressure ultrafiltration CuO/hydroxyethyl cellulose composite ceramic membrane for separation of Cr (VI) and Pb (II) from contaminated water. Chemical EngineeringJournal 336(2018) 570–578.

Crini, G and Lichtfouse E, Advantages and disadvantages of techniques used for wastewater treatment. Environmental Chemical Letter 17(2019) 145–155

Kalaiarasi S, Sivakumar A, Dhas S A M B, Jose M, Shock wave induced anatase to rutile TiO_2 phase transition using pressure driven shock tube, Material Letter 219(2018) 72-75

Das C, Patel P, De S, Das Gupta, S, Treatment of tanning effluent using nanofiltration followed by reverse osmosis. Separation and Purification Technology 50(2006) 291–299

Dixit S Yadav, V L, Optimization of polyethylene/polypropylene/alkali modified wheat straw composites for packaging application using RSM. Journal of Cleaner Production 240(2019) 118228

Gasemloo S, Khosravi M, Sohrabi MR, Dastmalchi S, Gharbani P, Response surface methodology (RSM) modeling to improve removal of Cr (VI) ions from tannery wastewater using sulphated carboxymethyl cellulose nanofilte. Journal of Cleaner Production 208(2019) 736-742.

Goyal RK, Jayakumar NS, Hashim MA, A comparative study of experimental optimization and response surface optimization of Cr removal by emulsion ionic liquid membrane. Journal of Hazardous Material 195(2011) 383-390.

Hudaya T, Marsha A, Paramita E, Shierin, Andrean D, Effect of pH and photocatalyst concentration on hexavalent Chromium Removal from Electroplating waste water by UV/TiO_2Photocatalysis. Journal of Applied Sciences 13(4) (2013) 639-644

Jyothi, MS, Vignesh, N, Mahesh P, Balakrishna, R G, Soontarapa, K, Eco-friendly membrane process and product development for complete elimination of chromium toxicity in wastewater. Journal of Hazardous Material 332(2017) 112–123.

Judai K, Iguchi N, Hatakeyama Y Low-Temperature Production of Genuinely Amorphous Carbon from Highly Reactive Nanoacetylide Precursors. Journal of Chemistry 2016 (2016) http://dx.doi.org/10.1155/2016/7840687.

Kazemi, M, Jahanshahi, M, Peyravi, M, Hexavalent chromium removal by multilayer membrane assisted by photocatalytic couple nanoparticle from both permeate and retentate. Journal of Hazardous Material 344 (2018) 12–22

Kumar, S, Mishra, D K, Sobral, A J F N, Koh J, CO_2 adsorption and conversion of epoxides catalyzed by inexpensive and active mesoporous structured mixed-phase (anatase/brookite) TiO_2 Journal of CO_2Utilization 34(2019)386-394

Liu, L, Xu, Y, Wang, K, Li, K, Xu, L, Wang, J, Wang, J, (2019)Fabrication of a novel conductive ultrafiltration membrane and its application for electrochemical removal of hexavalent chromium. Journal of Membrane Science584: 191-201.

Lu S.-Y, Qian, J.-Q,Wu Z.-G ,Ye W.-D, Wu G.-F, Pan Y.-B , Zhang K.-Y,Application of statistical method to evaluate immobilization variables of trypsin entrapped with sol-gel method. Journal of Biochemical Technology 1 (3) (2009) 79-84.

Meng, N, Priestley RCE, Zhang Y, Wang H, Zhang X, The effect of reduction degree of GO nanosheets on microstructure and performance of PVDF/GO hybrid membranes**.**Journal of Membrane Science 501(2016)169–178.

Mittal A, Naushad A, Sharma G, Alothman Z A, Wabaidur S M, Alam M, Fabrication of MWCNTs/ThO_2 nanocomposite and its adsorption behavior for the removal of Pb(II) metal from aqueous medium. Desalination and Water Treatment (2015) 21863-21869

Mohamed, A, Osman,TA, Toprak, MS, Muhammed, M, Yilmaz, E, Uheida, A, Visible light phoyocatalytic reduction of Cr(VI) by surface modified CNT/titanium dioxide composite nanofibre. Journal of Molecular Catalysis A: Chemical 424 (2016)45-53

Mohammed K and Sahu, O, Recovery of chromium from tannery industry waste water by membrane separation technology: Health and engineering aspects. Scientific African, 4(2019) e00096

Oh SJ, Kim N, Lee YT, Preparation and characterization of PVDF/TiO_2 organic–inorganic composite membranes for fouling resistance improvement. Journal of Membrane Science 345(2009) 13-20

Qamar M, Gondal MA, Yamani ZH, Synthesis of nanostructured NiO and its application in laser-induced photocatalytic reduction of Cr(VI) from water. Journal of Molecular Catalysis A: Chemical 341(2011)83–88

Ramasundaram S, Seid, M G, Choe, J W, Kim, E J, Chung, Y C, Cho, K, Lee, C, Hong, S W, Highly reusable TiO_2 nanoparticle photocatalyst by direct immobilization on steel mesh via PVDF coating, electrospraying, and thermal fixation. Chemical Engineering Journal 306(2016)344-351

Riaz T, Ahmad A, Saleemi S, Adrees M, Jamshed F, Hai AM, Jamil T, Synthesis and characterization of polyurethane-cellulose acetate blend membrane for chromium (VI) removal. Carbohydrate Polymer 153(2016)582–591.

Scholz WG, Rougé P, Bódalo A, Leitz U, Desalination of mixed tannery effluent with membrane bioreactor and reverse osmosis treatment. Environmental Science and Technology 39(21) (2005)8505-8511.

Tan I, Ahmad A, Hameed B, Optimization of preparation conditions for activated carbons from coconut husk using response surface methodology. Chemical Engineering Journal 137 (3)(2008) 462-470.

VenkataGiri, RK, Raju, LS, Nancharaiah, YV, Pulimi, M, Chandrasekaran, N, Mukherjee, A, Anaerobic nano zero-valent iron granules for hexavalent chromium removal from aqueous solution. Environmental Technology and Innovation 16(2019)16100495-100507

Sharma G, Naushad M, Muhtaseb A, Kumar A, Khan R, Kalia S, Bala M, Sharma A Fabrication and characterization of chitosan-*crosslinked*-poly(alginic acid) nanohydrogel for adsorptive removal of Cr(VI) metal ion from aqueous medium, International Journal of Biological Macromolecule 95(2017) 95484-493.

Zhang S, Shi Q, Korfiatis G, Christodoulatos C, Wang H, Meng X, Chromate removal by electrospun PVA/PEI nanofibres: Adsorption, reduction, and effects of co-existing ions, Chemical Engineering Journal 387 (2020) 124179-124188